Comparative Analysis of Fractal Properties of Solar Faculae

Sumbul Zehra,[1,2] * Saif Uddin Jilani [2]

[1] Department of Education and Literacy, Government of Sind, Karachi, Pakistan
[2] Department of Physics, University of Karachi, Karachi, Pakistan

*Email: znska@yahoo.com

Abstract: Present study is aimed at investigating the solar faculae area from 1990 to 2007 which partially covered the 22nd and 23rd solar cycle. Rescaled Range Analysis (RRA) and Detrended Fluctuation Analysis (DFA) have been adopted to evaluate the behaviour of nonlinear dynamics of solar faculae area. Results show that the value of Hurst exponent for solar faculae area from RRA and DFA is negatively correlated. It means it is non-persistent and long-range correlated. Obtained result is inaccurate so the only solution is to transform the data into stationary data by taking differencing. RRA is applied on residuals and RRA to evaluate the fractal property of the time series. Solar faculae area investigated in this study is fractal in nature and predictable ass well. Moreover, the time series of solar faculae area is non-linear as established by the Brock – Dechert – Scheinkman (BDS) test results.

Keywords: Fractal dimension, solar faculae area, rescaled range analysis, detrended fluctuation analysis, bds test and Kalman filter.

Introduction

Solanki (2009) and Keller et al. (2004) found that the bright region in the periphery of photospheric radiation is Solar Faculae. Benoit Mandelbrot was the first who introduced this term 25 years ago [9]. These are found near the solar limb as well as in the total zone of sunspots and are related to the magnetic field (Solanki, 2009; Keller et al, 2004). Most of the faculae occur in plages or fragments of active regions. Solar faculae existence have been shown when telescopes are pointed at the sun but it is not acertained. Slightly higher total solar irradiance at solar maximum is also due to the presence of faculae in abundance around sunspots (Fröhlich, 2002) . Due to such characteristics, solar faculae are more striking to study with other solar variables like sunspot numbers and solar flares and terrestrial or stratospheric variable like ozone etc. Kim et al. (2006) described fractal dimension as a quantitative parameter because it defines irregular time series characteristics. They used this parameter in the solar cycles to investigate different aspects of solar activity that are irregular in nature (R. S. Kim et al, 2006). Since fractals are infinitely complex patterns, these are known as pictures of chaos. Fractals are used to display image compressing of self-similar structures in nature. There are various objects like clouds, snowflakes, river network, the system of blood vessels, the growth pattern of bacteria, the pattern of situations like dendrites, etc. (Harrouni, 2003; Harrouni, 2002; Maafi, 2000; Maafi, 2003). As solar magnetic activity is governed by sunspots and solar faculae, fractals are used to study the irregular aspects of solar magnetic activity (Deng, 2015).

Fractal illustrates phenomena that are temporal and spatial in nature (Deng, 2015). Its shape is rough and can be further divided into parts where every part has the same properties as the whole. Consequently, fractal geometry came into existence to study the fractal shapes that look irregular and chaotic when compared with standard geometric shapes. However, it has been observed that fractal shapes show ordered behaviour because of their distinct property of invariance when they contract or expand (Deng, 2015). According to Fractal classification by Harrouni et al. (2008), fractals are those objects that present a high degree of geometrical complexity. Consequently, FD is used to describe and model fractals on different scales to show their geometrical irregularities. . The description and modelling of fractal objects are supported by using a dominant index called fractal dimension. . Fractal dimension is used to compare the two curves and their complexity (Harrouni et al, 2008). Present study is aimed at investigating the solar faculae area from 1990 to 2007 which partially covered the 22nd and 23rd solar cycle. Rescaled Range Analysis (RRA) and Detrended Fluctuation Analysis (DFA) have been adopted to evaluate the behaviour of nonlinear dynamics of solar faculae area.

Materials and Methods

The data of solar faculae area has been taken with consent from Kislovodsk mountain astronomical station of the Pulkovo observatory for the period from 1990 to 2007.

Detrended Fluctuation Analysis (DFA) and Rescaled Range Analysis (RAA) techniques are used to find the Hurst exponent of solar faculae area. Softwares used for analysis are, Minitab 17 (Barbara Falkenbach Ryan, Thomas A. Ryan, Jr., and Brian L. Joiner, Pennsylvania State University), R -package 3.2.5 (Bell Laboratories (formerly AT&T, now Lucent Technologies) by John Chambers and colleagues),

Statistica (STAT SOFT, USA) and EViews 6 (IHS Mar kit Ltd, London).

Fractal Dimension

In principle, the fractal dimension FD is given by

$$FD = - \log N (bx) / \ln (bx) \qquad (1)$$

Where, covering a structure of Euclidean dimension ED (1, 2, 3 for 1D, 2D, 3D structures, respectively) with boxes of size bx; N (bx) is the number of boxes that contain a part of the structure. The box-counting dimension, which is a practical application of the concept, is given by

$$BFD = - \lim (bx ->0) \log N (bx) / \log (bx) \qquad (2)$$

The randomness of a time series is determined by fractal dimensions which suggests if nature is chaotic or not of the physical structure. As the indicator of the interior solar structure is solar neutrino flux, so it is obvious to find the nuclear energy generation of the sun by studying the solar neutrino flux source so that it can help to determine whether the sun is fractal or not. This technique has suggested the rigid nature of solar features as solar faculae, solar flare etc. If FD of any physical structure is observed lying between1 to 2, it is classified as fractal and irregular in nature (Ghosh, 2020).

FD method is used to observe complexity and to prove that solar faculae area is fractal in nature. The relationship of FD and H as given by Das et al., (2009) is as follows:

$$FD = 2 – H \qquad (3)$$

The time-series data's dynamical behaviour is represented by FD and H.. Anti-persistent and persistent nature are mainly compared through Hurst exponent. In this study relation (1.2) will be used to analyse the nature of variables. The Fractal dimension tells the trend-reinforcing or persistent behaviour for FD < 1.5 which means that if there is an increase in the curve for a period then the increment will be continued for another period, and this could be considered as a biased random walk process. Also, the degree of persistence is dependent on the extent for H close to 1. However if FD >1.5 it shows an anti-persistent, ergodic, or mean-reverting behaviour, this means that a period of increases tends to show up after a period of decreases, thus the degree of anti-persistent depends on the extent for H close to 0.5.

After calculating FD, predictability indicators P is determined. Statistical relationship presented by Deng LH et al, 2015 is:

$$P = 2 (FD - 1.5) \qquad (4)$$

If the value of P is zero, then the system under consideration will not be predictable. Although, when the value of P becomes close to one, then that system that is dynamical is considered as a very predictable process.

The predictability P is close to zero when FD ~ 1.5, apparently for a Euclidean dimension ED=2.On the other hand, the system is predictable if P~1 occurs for FD ~ 2. This means that the system is predictable if a 2D structure is close to non-fractal.

Rescaled Range Analysis (RRA)

RRA analysis is applied to evaluate the fractal property of the time series and the long-range correlation. This analysis is simple but strong method for fast fractal analysis (Das, 2009).

This method evaluates the series that diverged from their mean (López-Montes et. al., 2012). Moreover, it can calculate Hurst Exponent (Krištoufek, 2010; KKW, 2014; Kannan, 2012). . The Hurst Exponent is the measure of the smoothness of fractal time series based on the asymptotic behaviour of the rescaled range of the process.

RAA analysis shows the difference of original time series from correlated time series (Peter, 1996; Peters, 1994).

Consider the time series $Z = \{ z_1.z_2, z_3, ..., z_N \}$ with complete size N such that N classifies further small samples (n) so that the series becomes accordingly as $N, \dfrac{N}{2}, \dfrac{N}{4}, \dfrac{N}{8}, ...$ and so on. The average rescaled range is then calculated for each value of n. The mean adjusted series (y (n)) (deviation of the time series Z_i from its mean $\bar{Z}$) can be proposed for eachvalue of n. The procedure for the rescaled range for a partial time series of length n is as follows,

Step: 1 Computed mean ($\bar{Z}$) and adjusted cumulative series y (n) for i=1, 2, 3 …n,

$$y (n) = \sum_{i=1}^{N}[z_i - \bar{z}] \qquad (5)$$

Where Z_i = original time series data, $\bar{Z}$ = mean and N is discrete-time.

Step: 2 Find range (R)

$$R(N) = \max.y(N) - \min.y(N) \qquad (6)$$

Step: 3 Calculated Standard Deviation (S) as follow

$$S(N) = \sqrt{\dfrac{\sum_{i=1}^{N}[z_i - \bar{z}]^2}{N-1}} \qquad (7)$$

Step: 4 The Rescaled range is then computed from step 2 and 3 and the average of overall partial time series of length n.

$$R/S = \frac{\max.y(N) - \min.y(N)}{\sqrt{\dfrac{\sum\limits_{i=1}^{N}[z_i - \bar{z}]^2}{N-1}}} \quad (8)$$

Step: 5 Compute Hurst exponent (H)

Suppose the range (R) of given time-series data that is dependent on a sequence of arbitrary variables has a fixed standard deviation (S), Both R and S will be independent. The ratio R/S will follow a power law given as:

$$R/S\alpha(N)^H \quad (9)$$

Applying log on both sides, we have:

$$H = \frac{\log_2(R/S)}{\log_2(N)} \quad (10)$$

By applying the least square procedure against log_2 (R/S) vs. log_2 (N), the slope of the best-fitted curve will determine the value of H (Kale MD,2005).

The procedure is repeated for whole samples (n) over the time series data and dividing each sample interval by two and determining R/S for each sample (n) which is shown in figure 1 the slope of the best-fitted curve gives the value of H=0.30 of solar faculae which are shown in equation y = 0.3x + 0.57. AR (p) residuals are estimated before R/S analysis and applied on data of ozone by Weng to remove linear dependency (wengYC,2008).
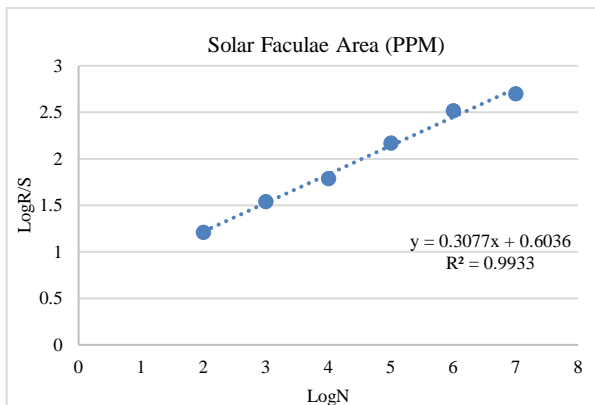
Fig. 1 Plot of log (r/s) vs. log (n) of rescaled ranged analysis of solar faculae area whose fitted line slope evaluates the hurst exponent for the year from 1990 to 2007.

Unit Root Test is also used to find the stationarity of the variable as RRA is applied on stationary time series.

Detrended fluctuation analysis (DFA)

Detrended Fluctuation Analysis is applied to the time-series data to calculate interrelated properties that are extracted from various structures [23,31]. To determine DFA, considering the time series {Ui} i = 1, 2, 3 … N, where N is the size of Faculae area data series. The following steps will determine DFA:
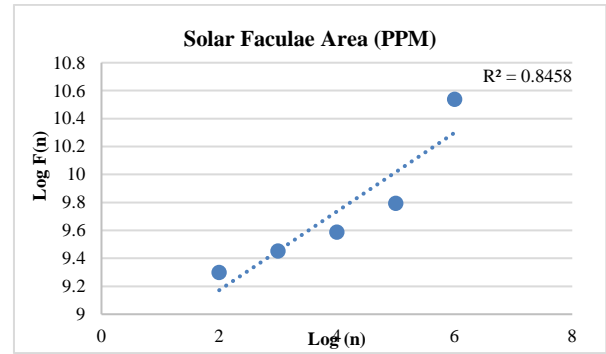
Fig 2 Plot of Log F (n) vs. Log (n) of Solar Faculae area of Detrended Fluctuation Analysis.
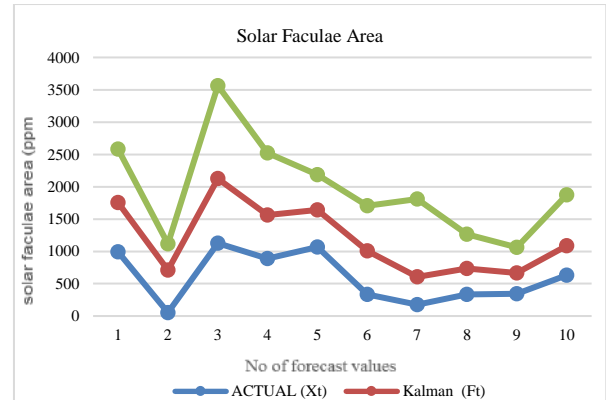
Fig. 3 Plot of actual, forecast and kalman values of solar faculae area.

H(n) the time series is determined by:

$$H(n) = \sum_{i=0}^{n}(U_i - \bar{U}) \quad (11)$$

Where $\bar{U}$ represent the mean value

The least-square procedure is applied to each segment. Each segment is obtained by dividing the series into boxes of equal sizes.

To detrend every segment, subtract $\hat{H}(n)$ from H(n):

$$H(n) - \hat{H}(n) \quad (12)$$

The following relation is used to find RMS variation between Detrended and original time series:

$$H(n) = \sqrt{\frac{1}{N}\sum_{i=1}^{N}\left[H(n) - \hat{H}(n)\right]^2} \quad (13)$$

Hurst exponent α is determined by:

$$H(n) \sim n^\alpha \quad (14)$$

To get the relationship between H (n) and n, the above steps must be applied to all parts (Zhang, 2011). The graph between H (n) and n formed (shown in figure 3) the slope will be called as Hurst exponent which is denoted by 'α'. If the value of α is 0, then no significant correlation is found. If it is > 0.5 then the correlation is positive while if < 0.5 it is said to be anti-correlated in the original time series (Bashan et. al., 2008; Jan et. al., 2018).

If forecast period is denoted by F_t in period t, and new knowledge is denoted by X_t then forecast period t + 1 is expressed as

$$F_{t+1} = \frac{\sigma_F^2 X_t + \sigma_X^2 F_t}{\sigma_F^2 + \sigma_X^2} \tag{15}$$

$$\sigma_a^2 = \sum_{t=2}^{n} \alpha_t^2 = \frac{RSS}{N} \tag{16}$$
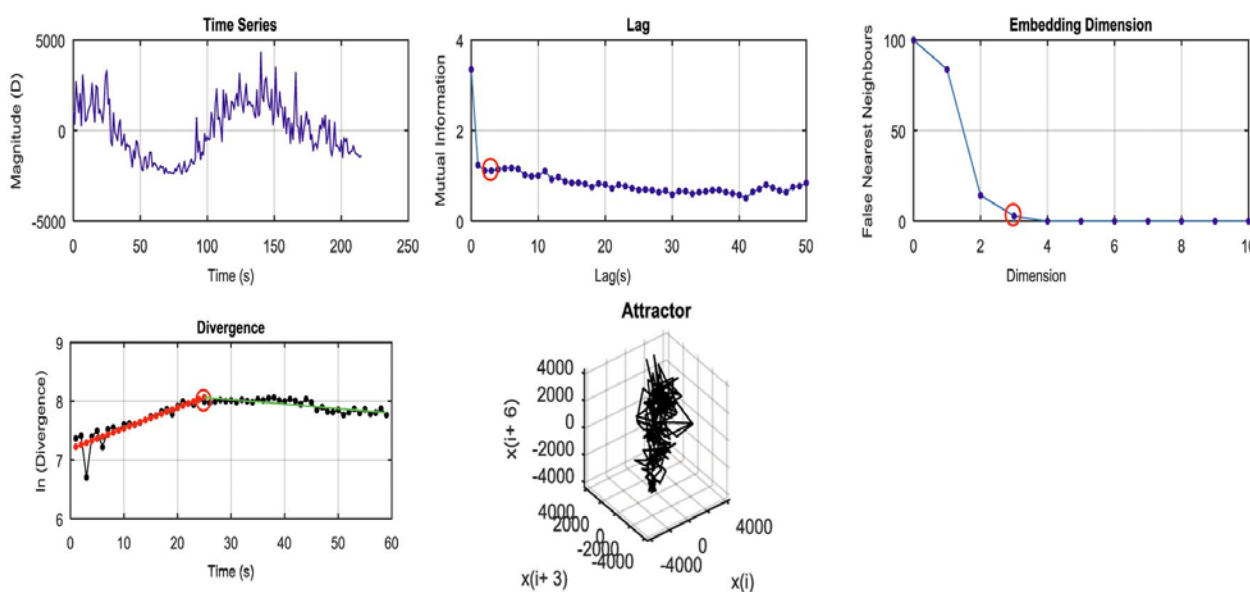
Fig. 4 chaos theory results for each processing step for solar faculae. 4a detrended accommodation time trace. 4b mutual information. The first minimum is the embedding lag which is five data points. 4c the percentage of false nearest neighbors versus embedding dimension. The dimension is three in this case as this results in ≤5% false nearest neighbors. 4d the time evolution of the average separation of nearby trajectories in phase space. The slope of the linear rise is the le. The end of the linear rise is the limit of predictability. 4e the reconstructed phase.

The BDS test

BDS is a strong tool that distinguishes independent series from original series because time series are highly irregular (Akintunde etal ,2015). Since BDS test is two-tailed, the test statistic is less than the negative critical z-value or higher than the positive critical z-value, the null hypothesis will be rejected. For example, α = 0.05, the critical z-value = ±1.96.

H_0: linearly dependent series

H_1: non-linearly dependent series (Akintunde et. al., 2015).

Kalman Filter

Kalman filter is applied to evaluate the forecasted values of the fitted models so the errors can be reduced. Kalman filtering is an approach that uses two independent values to form a weighted value of the forecast. One value is based on previous knowledge and the other is based on new knowledge. Thus, the Kalman filter works to combine these two pieces of values to extract an enhanced and upgraded forecast value.

Where,

RSS = residual sum of squares

N = number of residuals

Kalman filter is used because it allows non-stationary data to be implemented (Gough et. al., 1992; Shanmugan et al, 1988).

Largest Lyapunov Exponent

The positive largest Lyapunov exponent (LE) is a marker of chaos, which also means dependent sensitivity on initial conditions (Rosenstein MT,etal, 1993). . In phase space, the distance between nearby trajectories change exponentially over time is described by LE. Custom code in MATLAB (Math Works, Massachusetts, USA) is used to carry out all the processing. The linear trend in the data was removed before carrying out any calculation of any parameter related to chaos theory analysis (Williams et. al., 1997). The LE was calculated through the use of an algorithm (Rosenstein et. al., 1993) which is suitable for small data sets and robust to noise. The resulting slopes of the largest Lyapunov exponent for

the time series are determined through the least-squares line fitting method. These are found through the reasonable values of the largest Lyapunov exponent which is LLE = 0.0351

Results and Discussion

The FD is not dynamical but a statistical quantity that measures the dynamical complexity of the chaotic time series. RRA analysis is used to estimate the nonlinearity of solar faculae. The nonlinear dynamics of the solar faculae area has been investigated using RRA analysis and DFA methods in this investigation. The FD of solar faculae area obtain from both methods have been illustrated in "Table 2" and "Table 3". It recognises that the solar faculae area is anti- persistent in nature as their FD is 1.70 and 1.76 from RRA analysis and DFA methods respectively.

zero indicating that the variable is predictable in nature.

Table8 for BDS test shows that test statistics is less than the critical values (±1.96). Consequently, the null hypothesis is neglected for the linear dependency of the series.and the solar faculae area is non-linearly dependent. Before fitting the model, the stationarity has been checked out out (Jan et. al., 2018; Akintunde et. al., 2015; Wang et. al., 2006; Özer et. al., 2010).

Augmented Dickey-Fuller statistics is used to apply the Unit Root Test on the time series to confirm their stationarity (Akintunde et. al., 2015).Unit root test is applied on solar faculae area to confirm their stationarity as shown in Table 7.This shows that statistical levels have exceeded the critical value. Thus, clarifies the stationarity of the series at the first

Table 1 Hurst Exponent and Fractal Dimension Relationship.

FD	H	Nature of Process	Correlation
>1.5	<0.5	Anti-persistent	Negative
=1.5	=0.5	Brownian	Zero
<1.5	>0.5	Persistent	Positive

Table 2 Fractal Dimensions and Hurst Exponent of Solar Faculae Area obtained by R/S analysis

Variables	Fractal Dimension	Hurst Exponent	Predictability indicator	Model	R^2
Solar Faculae Area	1.70	0.30	0.40	ARIMA (5,1,8)	75%

Table 3 Fractal Dimensions and Hurst Exponent of Solar Faculae Area obtained by Detrended fluctuation analysis.

Variables	Fractal Dimension	Hurst Exponent	Predictability indicator
Solar Faculae Area	1.76	0.24	0.52

Table 4 R/S analysis of Solar Faculae Area.

size (N)	Xmax	Xmin	R	S	R/S	LOG N	LOG (R/S)
128	2482.7	-2330.5	4813.2	739.4	6.51	7	2.7
64	2310	-2330	4641	804	5.772	6	2.52
32	2310	-2330	4641	1028	4.51	5	2.17
16	2310	-1263	3573	1025	3.48	4	1.79
8	2310	-1263	3573	1222	2.92	3	1.54
4	1830	-740	2570	1114	2.31	2	1.21
H	0.30						
FD	1.70						

Since FD represents the roughness and the Hurst exponent represents the smoothness of the data, the Hurst exponent is attained to detect more accurate, persistent and smooth variable. Table 1" depicts H for smoothness from which it is investigated that solar faculae area is smooth. It is clear from Table 2 and 3 that the fractal dimension of solar faculae area lies between 1 and 2 (as stated by Ghosh, 2006 on the data of solar neutrino flux) from which it concluded that solar faculae area are fractal in nature because their FD is 1.70.

The predictability indicator value of the solar faculae area is greater than zero indicating that the variable is predictable in nature. The predictability indicator value of solar faculae area is 0.40 and 0.52 by RRA analysis and DFA method respectively which is greater than

difference, so our time series is non-stationery.

In this investigation, Hurst exponent of solar faculae area is obtained through RRA analysis where AR (5,1,8) residuals are used because it formed the best-fitted model. The coefficient of determination (R^2) of this model is obtained as 75% and its forecast equation is also shown below which is generated from values of "Table 10".This calculated value of solar faculae area matched with the forecast value of the ARIMA model, shown in Table 9. Table 4 shows the whole procedure by taking different residual samples. When the slope of the best-fitted line is taken between log N and log (R/S) then Hurst exponent (H = 0.31) is obtained which is indicated in Figure 1. Moreover, equation (3) is used to get FD = 1.70. Hence, it is proved by determining FD and H that the solar faculae area data

is anti-persistent because H is less than 0.5 and FD is greater than 1.5 and it is long-range correlated.

"Table 5" presents the correlated properties of the Solar Faculae Area which is the purpose of DFA. Equations (13) and (14) are used to assess these results. The value of the Hurst Exponent is 0.24.

trend altogether thus to avoid misleading results detrending and differencing must be applied to remove deterministic trend and variance respectively. (Matos et. al., 2004).

If the relationship between actual and forecasted values is strong then the model is exemplified as the best fit.

Table 5 Detrended fluctuation analysis for Solar Faculae Area.

H estimate	0.24			
Domain	Time			
Statistic	RMSE			
Length of series	215			
Block detrending model	x ~ 1 + t			
Block overlap fraction	0			
Scale ratio	2			
Scale	4.0000	8.0000	16.0000	32.000	64.0000
RMSE	630.47	701.53	769.82	888.57	1487.5

Table 6 Estimated Detrended fluctuation Analysis of log F(n) vs. log (n) of Solar Faculae Area from 1990 to 2007.

Level	(n)	F(n)	$\log_2(n)$	$\log_2 F(n)$
1	64	1487.5	6	10.54
2	32	888.57	5	9.79
3	16	769.82	4	9.59
4	8	701.53	3	9.45
5	**4**	**630.47**	**2**	**9.30**

Table 7 Unit Root Test of Solar Faculae Area.

AT LEVEL:

		t-Statistic	Prob.*
Augmented Dickey-	Fuller test statistics	-2.29	0.43
Test critical values:	1% level	-4.00	
	5% level	-3.43	
	10% level	-3.14	

AT FIRST DIFFERENCE:

		t-Statistic	Prob.*
Augmented Dickey-	Fuller test statistics	-17.34	0.0000
Test critical values:	1% level	-4.00	
	5% level	-3.43	
	10% level	-3.14	

Moreover, equation (3) is used to get FD = 1.76. Table 6 presents the estimated result for DFA of the solar faculae area. The best-fitted line slope is calculated by log n vs. log F (n) line, s is shown in Figure 2. Thus, DFA also proves that solar faculae area data is anti-persistent because H is less than 0.5 and FD is greater than 1.5.

As RRA analysis is done on stationary time series, its results are more accurate than DFA. Unit root test identified the data of solar faculae as non-stationary, the result obtained is inaccurate so the only solution is to transform the data into stationary data. Also, if the time series data show a deterministic trend, the inaccurate and poor results can be avoided by detrending and transformation from non-stationary to stationary process can be done by differencing that's why RRA is applied on residuals. Sometimes, the time-series data show stochastic and deterministic

To check this relationship select 200 values out of 216, and fit the model on 200 values and forecast the next 10 values. Forecast values of solar faculae area are generated from Statistica software ("As shown in Table 9") after being corrected with a Kalman filter. From (Table 9, Figure 3) compares the predicted and actual future values. This purpose is estimated to confirm if the model minimizes the difference between actual values and the forecasted values of data points.

Variations in solar radiations reaching the earth are due to a balance between decreases caused by sunspots and increases caused by bright areas called faculae which surround sunspots, so to check the variability of solar faculae it has been forecasted(D'Aleo et. al., 2016) .

Tests for the dependence of nonlinearity

The results from table 8 suggest that the solar faculae area has non-linear dependence because the value of

Table 8 BDS Test of Solar Faculae Area.

Dimension	BDS Statistic	Std. Error	z-Statistic	Prob.
2	0.09	0.003	27.74	0.00
3	0.16	0.005	29.10	0.00
4	0.21	0.007	32.01	0.00
5	0.24	0.007	34.78	0.00
6	0.26	0.007	38.55	0.00

Table 9 Forecast Cases and Kalman Correction for Solar Faculae Area (5, 1, 8).

Case No:	Actual (X_t)	Forecast (F_t)	Corrected values (F_{t+1})	Lower 90.0000% (F_t)	Upper 90.0000% (F_t)	Std.Err. (F_t)
201	993	710.1544	763.6753846	-622.52	2042.834	806.154
202	54	798.4592	657.5900826	-610.80	2207.715	852.476
203	1126	968.5504	998.3435817	-456.63	2393.729	862.109
204	889	624.3120	674.3971445	-842.69	2091.314	887.408
205	1068	458.2605	573.6374777	-1028.88	1945.400	899.589
206	334	753.3369	673.9885461	-743.69	2250.361	905.568
207	178	485.4493	427.2727212	-1056.43	2027.329	932.702
208	335	414.3572	399.3409975	-1182.26	2010.978	965.816
209	346	316.5365	322.1116736	-1336.79	1969.863	1000.117
210	631	417.2732	457.7153084	-1266.94	2101.486	1018.801

Table 10 Parameters for model equation of Solar Faculae Area (5, 1, 8).

Estimate constant	$\phi1$	$\phi2$	$\phi3$	$\phi4$	$\phi5$	-	-	-
-14.8010	-0.9654	-0.5145	0.2974	0.6508	0.7932	-	-	-
_	$\Theta1$	$\Theta2$	$\Theta3$	$\Theta4$	$\Theta5$	$\Theta6$	$\Theta7$	$\Theta8$
_	-0.3092	0.3034	0.7115	0.5308	0.3884	-0.6660	-0.2525	-0.1064

the BDS test concerning each dimension lies within the critical region. Therefore, the null hypothesis is being rejected. This is one of the indications of the fractal nature of the solar faculae area. Tamil et. al. (2015) investigated in their paper that sunspot number is dynamic in nature and have a low-dimensional chaotic attractor and solar activity is a chaotic phenomenon. They proved this nature with different nonlinear dynamic methods, with varying levels of complexity. These dynamic nonlinear methods are average mutual information and embedding dimension method and the correlation dimension method. These methods have identified chaotic behaviour in the sunspot number and solar activity is a chaotic phenomenon. Furthermore, as solar activity is governed by chaotic attractor and sunspots and solar faculae both are parts of solar activity and our time series is long-range correlated it is stochastic not chaotic in nature as proved by the value of the largest Lyapunov exponent (Qin, 1998).

Largest Lyapunov Exponent

In figure 4, the plot shows variations of the divergence as a function of the time interval for solar faculae. This figure also shows the profiles of the curve that shows linear increases and in comparison flat regions with some fluctuations that are superimposed on the part of the curves. The resulting slopes of the largest Lyapunov exponent for the three-time series are determined through the least-squares line fitting method. These are found through the reasonable values of the largest Lyapunov exponent which is LLE = 0.0351

The information theory method, claims that the largest Lyapunov exponent will result in the more complex dynamical behaviour of the system. The results of this study show that the dynamic behaviour or the chaotic degree of the solar faculae is not complex.

As sunspots and solar faculae, both are the parts of solar activity cycle and there is a highly significant negative correlation between the relative sunspot numbers and the total atmospheric ozone. (Willett, 1962) So solar activity can cause the ozone levels in the upper stratosphere to be substantially depleted, but since most of the ozone is in the middle stratosphere, the effect on the total ozone column is negligible. There is only 0.1 % more UV radiation at the sunspot maximum than at minimum which causes only a 2% change in ozone concentrations.

Similar to sunspots, faculae are also concentrations of magnetic field lines, but their diameter is much smaller than a few hundred kilometres. This difference in size produces a very important change. Instead of blocking energy, like sunspots, faculae transport energy more efficiently to the Sun's surface. This results in faculae being brighter than the rest of the Sun's surface. In general, the faculae's brightness is enough to overcompensate for the local darkening of the sunspots. Therefore, the Sun is brighter at maximum activity. As there is only 0.1% more UV radiation received at sunspots maximum this variation is very small. However, in some specific parts of the light spectrum, such as in the near- and mid-ultraviolet, the variation can be much larger from 1 – 10% in the ultraviolet

(Shindell, 1999) . So solar faculae have much impact on ozone layer depletion as compare to sunspots.

Model Equation

$$\hat{Y}_t = \mu + Y_{t-1} + \Phi_1 (Y_{t-1} - Y_{t-2}) + \Phi_2 (Y_{t-2} - Y_{t-3}) + \Phi_3 (Y_{t-3} - Y_{t-4}) + \Phi_4 (Y_{t-4} - Y_{t-5}) + \Phi_5 (Y_{t-5} - Y_{t-6}) - \theta_1 e_{t-1} - \theta_2 e_{t-2} - \theta_3 e_{t-3} - \theta_4 e_{t-4} - \theta_5 e_{t-5} - \theta_6 e_{t-6} - \theta_7 e_{t-7} - \theta_8 e_{t-8}$$

$\hat{Y}_{201}$ = -14.8010 + 393 + (-0.9654) (393 – 563) + (-0.5145) (563 – 739) + (0.2974) (739 – 704) + (0.6508) (704 – 2008) + (0.7932) (2008 – 756) – (-0.3092) (-260.59) – (-0.3034) (-647.00) – (0.7115) (-474.43)– (0.5308) (-505.59) – (0.3884) (808.01) – (-0.6660) (-148.35) – (-0.2525) (-1022.38) – (-0.1064) (-1176.89) $\hat{Y}_{201}$ = 713.36 655

Conclusion

It has been recognised that FD for solar faculae area is anti-persistent in nature. The FD-H analysis also verifies that the solar faculae area is fractal in nature. Additionally, the solar magnetic activity cycle is fractal in nature as indicated by long-range correlation. DFA analysis is found more suitable for non - stationary time series as compared to RRA for stationary time. Solar faculae area found to be non - stationary as depicted by Unit Root Test but the result obtained is inaccurate so the only solution is to transform the data into stationary data which is done by differencing. Hence, RRA is more suitable for estimating the parameters of solar faculae area. Linearity is rejected by the BDS test application and proves that the time series is non-linear. Results of present study suggest that the dynamic nonlinear behaviour of the solar faculae is stochastic not chaotic and complex . Value of the largest Lyapunov exponent for solar faculae area is LLE = 0.0351which proves that solar faculae area is not chaotic. It is also deduced that solar faculae has more impact on ozone depletion than sunspot number because of variation in solar activity cycle found in the upper stratosphere.

Acknowledgement

References

Akintunde, M. O., Oyekunle, J. O., Olalude, G. A. (2015). Detection of non-linearity in the time series using BDS test. *Science Journal of Applied Mathematics and Statistics*, **3** (4), 184-192.

Barnsley, M. F. (1993). Measures on Fractals, In Fractals Everywhere, Elsevier. 330–378.

Bashan, A., Bartsch, R., Kantelhardt, J. W., Havlin, S. (2008). Comparison of detrending methods for fluctuation analysis. *Physica A: Statistical Mecha nics and its Applications*, **387** (21), 5080-5090.

Brown, R. G., Hwang, P. Y. (2012). *Introduction to random signals and applied Kalman filtering: with MATLAB exercises*. J Wiley & Sons.

D'Aleo, J.S. (2016). Solar changes and the climate, In Evidence-Based Climate Science: Data Opposing CO$_2$ Emissions as the Primary Source of Global Warming: Second Edition, Elsevier Inc., 263–282.

Das, N. K., Sen, P., Bhandari, R. K., Sinha, B. (2009). Nonlinear response of radon and its progeny in spring emission. *Applied Radiation and Isotopes*, **67** (2), 313-318.

Deng, L. H., Li, B., Xiang, Y. Y., Dun, G. T. (2015). Comparison of chaotic and fractal properties of polar faculae with sunspot activity. *The Astronomical Journal*, **151** (1), 2.

Falconer, K. (2004). *Fractal geometry: mathematical foundations and applications*. John Wiley & Sons.

Fröhlich, C. (2002). Total solar irradiance variations since 1978. *Advances in Space Research*, **29** (10), 1409-1416.

Ghosh, K., Raychaudhuri, P. (2006). Fractal Nature of Solar Interior. *arXiv preprint hep-ph/0605043*.

Ghosh, O., Ghosh, T., Chatterjee, T. N. (2014). Multi-technique analysis of the solar 10.7 cm radio flux time-series in relation to predictability. *Solar Physics*, **289** (6), 2297-2315.

Gough, K. (1992). Statistical Theory and Modelling. in Honour of Sir David Cox, Frs. **(41).** 244. doi: 10.2307/2348259..

Hanslmeier, A., Lemmerer, B., Utz, D., Muller, R., Muthsam, H. (2014). Fractal Dimension Analysis of Solar Granulation-Boxcounting dimension. *Central European Astrophysical Bulletin*, **38** (1), 11-17.

Harrouni, S. (2008). Fractal classification of typical meteorological days from global solar irradiance: Application to five sites of different climates. In *Modeling Solar Radiation at the Earth's Surface* (pp. 29-54). Springer, Berlin, Heidelberg.

Harrouni, S., Guessoum, A. (2003). Fractal Classification of solar irradiances into typical days using a cumulative distribution function. *ICREPQ '03, Vigo (Spain)*.

Harrouni, S., Maafi, A. (2002). Classification des éclairements solaires à l'aide de l'analyse fractale. *Revue Internationale des éenergies renouvelables*, **5**, 107-122.

Hassan, D., Abbas, S., Ansari, M. R. K., Jan, B. (2014). Solar flares data analysis on application of probability distributions and fractal dimensions and a comparative analysis of North-South Hemispheric solar flares data behavior. *Proceedings of the Pakistan Academy of Sciences*, **51** (4), 345-353.

Jan, B., Zai, M. A. K. Y., Afradi, F. K., Aziz, Z. (2018). Study nonlinear dynamics of stratospheric ozone concentration at Pakistan Terrestrial region. *Journal of Atmospheric and Solar-Terrestrial Physics*, **168**, 48-57.

Kale, M. D., & Butar, F. B. (2005). *Fractal analysis of time series and distribution properties of Hurst exponent* (Doctoral dissertation, Sam Houston State University).

Kim, R. S., Yi, Y., Cho, K. S., Moon, Y. J., Kim, S. W. (2006). Fractal Dimension and Maximum Sunspot Number in Solar Cycle. *Journal of Astronomy and Space Sciences*, **23** (3), 227-236.

KKW. Environment and undefined (2014). Statistical analysis of hourly surface ozone concentrations in Cairo and Aswan/Egypt.

Krištoufek, L. (2010). Rescaled range analysis and detrended fluctuation analysis: Finite sample properties and confidence intervals. *Czech Economic Review*, **4** (03), 315-329.

Lopez-Montes, R., Araujo-Pradere, E., Perez-Enriquez, R., Lopez Cruz-Abeyro, J. A. (2012). The impact of intense geomagnetic storms on the ionosphere at mid latitudes. *39th COSPAR Scientific Assembly*, **39**, 1109.

Maafi, A., Harrouni, S. (2000, January). Measuring the fractal dimension of solar irradiance in view of pv systems performance analysis. *In World Renewable Energy Congress VI* (pp. 2032-2035). Pergamon.

Maafi, A., Harrouni, S. (2003). Preliminary results of the fractal classification of daily solar irradiances. *Solar Energy*, **75** (1), 53-61.

Matos, J. M. O., Moura, E. P. De., Krüger, S. E., Rebello, J. M. A. (2004). Rescaled range analysis and detrended fluctuation analysis study of cast irons ultrasonic backscattered signals, Chaos, Solutions and Fractals, (**19**), 55–60. doi: 10.1016/S0960-0779 (03)00080-8.

Matsoukas, C., Islam, S., Rodriguez-Iturbe, I. (2000). Detrended fluctuation analysis of rainfall and streamflow time series. *Journal of Geophysical Research. Atmospheres*, **105** (D23), 29165-29172.

Özer, G., Ertokatlı, C. T. (2010). Chaotic processes of common stock index returns: An empirical examination on Istanbul Stock Exchange (ISE) market. *Available at SSRN 1617929*.

Peng, C. K., Buldyrev, S.V., Havlin, S., Simons, M., Stanley, H. E., Goldberger A. L. (1994). Mosaic organization of DNA nucleotides, Physics Reviews, (49). 1685–1689, doi: 10.1103/PhysRev E.49.1685.

Perakakis, P. (2009). Fractal analysis of cardiac dynamics: the application of detrended fluctuation analysis on short-term heart rate variability.

Peters, E. E. (1994). Fractal market analysis: applying chaos theory to investment and economics. **24,** John Wiley & Sons.

Peters, E. E. (1996). Chaos and order in the capital markets: a new view of cycles, prices, and market volatility. John Wiley & Sons.

Qin, Z. (1998). The transitional time scale from stochastic to chaotic behavior for solar activity. *Solar Physics*, **178** (2), 423-431.

Rosenstein, M. T., Collins, J. J., De Luca, C. J. (1994). Reconstruction expansion as a geometry-based framework for choosing proper delay times. *Physica D: Nonlinear Phenomena*, **73** (1-2), 82-98.

Selvi, S.T., Selvaraj, R.S. (2015). Investigation of Chaotic Nature of Sunspot Data by Nonlinear Analysis Techniques, undefined.

Shanmugan, K. S., & Breipohl, A. M. (1988). *Random signals: detection, estimation and data analysis.* Wiley.

Shindell, D., Rind, D., Balachandran, N., Lean, J., Lonergan, P. (1999). Solar cycle variability, ozone, and climate. *Science*, **284** (5412), 305-308.

Suresh Kannan, V. M., Inbanathan, S. S. R. (2012). Fractal dimensional analysis of ozone in tropical region. *International Journal of Current Research*, **4** (12), 129-130.

Teegavarapu, R. S., Chandramouli, V. (2005). Improved weighting methods, deterministic and stochastic data-driven models for estimation of missing precipitation records. *Journal of Hydrology*, **312** (1-4), 191-206.

Thomas, J. H., Weiss, N.O. (2008). Introduction to random signals and applied Kalman filtering: with Matlab exercises (Vol. 4). New York, NY, USA:

Weng, Y. C., Chang, N. B., Lee, T. Y. (2008). Nonlinear time series analysis of ground-level ozone dynamics in Southern Taiwan. *Journal of Environmental Management*, **87** (3), 405-414.

Willett, H. C. (1962). The relationship of total atmospheric ozone to the sunspot cycle. *Journal of Geophysical Research*, **67** (2), 661-670.

Zarger, R., Stepp, J. (2004). Persistence of botanical knowledge among Tzeltal Maya children. *Current Anthropology*, **45** (3), 413-418.

Zhang, Q., Zhou, Y., Singh, V. P., Chen, Y. D. (2011). Comparison of detrending methods for fluctuation analysis in hydrology. *Journal of Hydrology*, **400** (1-2), 121-132.